

COMPARATIVE STUDIES ON CONSTITUTIVE MODELS FOR COHESIVE INTERFACE CRACKS OF QUASI- BRITTLE MATERIALS

Xinpu SHEN

*College of Architectural Engineering,
Shenyang University of Technology*
Fax: 0086 24 2568 4990
E-mail: xinpushman@vip.sina.com

Guoxiao SHEN

*College of Architectural Engineering,
Shenyang University of Technology*
Fax: 0086 24 2568 4990
E-mail: guoxiaoshen_sut@sina.com

Lin ZHOU

College of Architectural Engineering, Shenyang University of Technology
Fax: 0086 24 2568 4990
E-mail: linzhou_sut@sina.com

ABSTRACT

In this paper, Concerning on the modelling of quasi-brittle fracture process zone at interface crack of quasi-brittle materials and structures, typical constitutive models of interface cracks were compared. Numerical calculations of the constitutive behaviours of selected models were carried out at local level. Aiming at the simulation of quasi-brittle fracture of concrete-like materials and structures, the emphases of the qualitative comparisons of selected cohesive models are focused on: (1) the fundamental mode I and mode II behaviours of selected models; (2) dilatancy properties of the selected models under mixed mode fracture loading conditions.

Keywords: Mixed-mode crack; plasticity; constitutive model; cohesive interface crack; quasi-brittle fracture.

1. INTRODUCTION

In the last decade, many researches have been devoted to analysis of the fracture of cement-based materials, subjected to either pure tension or mixed-mode fracture loading (see Bazant, Cedolin, 1991; Karihaloo, 1995). These models can be used in modelling of fracture process at the interface of two dissimilar materials, and can also be adopted in simulation of joint behaviour related to either masonry or grouted joints. Cohesive interface crack models for simulation of fracture process in frictional concrete-like materials consist of the following two fundamental features: (1) linear-elastic material behaviour is assumed throughout the considered solid or structure except at the locus of potential discontinuity, (2) displacement discontinuity is allowed over that locus and is related to traction across it by a suitable relationship. A review updated to 1991 of abundant literature concerning cohesive crack model can be found in Bazant and Cedolin (1991) and more can be found in Karihaloo (1995).

According to the experimental data reported by Hassanzadeh (1990) and Vutukuri, Lama and Saluja (1974), a practical cohesive interface model for concrete-like materials should have, at least, the following principal properties: (1) the ability of reproducing the gradual softening of material properties, (2) reproducing the phenomenon of finite dilatancy, (3) reproducing the phenomenon of Coulomb-type frictional behaviour. And more, the degradation of stiffness during unloading (crack closure) is also a pertinent aspect of an interface model.

In the following Section 2, typical formulations of constitutive models that concern modelling of fracture process zone at interface of structures and materials as quasi-brittle material are reviewed and compared. In Section 3, corresponding numerical tests are performed and solutions are compared. Emphases of the qualitative

comparisons of selected cohesive models are focused on: (1) the fundamental mode I and mode II behaviours of selected models; (2) dilatancy properties of the selected models under mixed mode fracture loading conditions.

For the purpose of extensivity, not only the existing cohesive interface models for concrete-like materials but also those for metallic materials and composites are explored in this study. Three classes of cohesive interface models are compared in the following contexts: (1) the models that have explicit expressions of $\mathbf{p-w}$ law (i.e. the traction-crack opening law) (see Camacho and Ortiz, 1996; Xu and Needleman, 1994) proposed mainly for quasi-brittle fracture of metallic materials; (2) the Coulomb type models with non-associate flow rule and a particular dissipation potential (Lotfi and Shing, 1994; Carol, Prat and Lopez, 1997; Cocchetti Maier and Shen, 2002; Shen, 2001), proposed mainly for quasi-brittle fracture in concrete-like materials; (3) Corigliano-Bolzon's interface model for quasi-brittle fracture in composites (Corigliano, 1993; Bolzon and Corigliano, 1997).

2. COHESIVE MODELS FOR MIXED-MODE INTERFACE FRACTURE

Definitions of interface variables for a mixed-mode cohesive fracture are given as follows: \mathbf{p} represents the traction vector on the interface and $\mathbf{p}=\mathbf{p}^+=\mathbf{p}^-$, \mathbf{u}^+ and \mathbf{u}^- the displacement vectors on two sides of the interface, respectively, and \mathbf{w} represents vector of crack opening, i.e., displacement discontinuity across the interface.

$$\mathbf{p} = \{p_n \mathbf{p}_t\}^T, \quad \mathbf{w} = \mathbf{u}^+ - \mathbf{u}^- = \{w_n \mathbf{w}_t\} \quad (1)$$

where p_n is normal traction component, \mathbf{p}_t is tangential traction vector, w_n is the normal component of crack opening, \mathbf{w}_t is tangential vector of crack opening. In problems considered here, deformation is assumed as small, in the sense that equilibrium relations are not influenced by configuration changes. And also it is assumed the mechanical process is an isothermal process.

2.1 Interface Model with Explicit $\mathbf{p-w}$ Relationship: Xu-Needleman Model for Mixed-mode Fracture

Because of its simplicity, the cohesive interface models with explicit $\mathbf{p-w}$ relationships were used by a few researches for the specialized applications at which the loading path and unloading process are not considered. Among them, the *Xu-Needleman* model is the representative one.

Based on thermodynamics laws, Xu and Needleman (1994) proposed their model for mode I and II mixed-mode fracture. The general $\mathbf{p-w}$ law is given as

$$\mathbf{p} = \begin{Bmatrix} p_n \\ p_t \end{Bmatrix} = \frac{\partial \phi}{\partial \mathbf{w}} \quad (2)$$

Free energy function on the interface proposed by Xu and Needleman [6] is

$$\phi(\mathbf{w}) = W_1 \left\{ 1 + \exp\left(-\frac{w_n}{w_{nc}}\right) \left[\left(1 - r + \frac{w_n}{w_{nc}}\right) \frac{1-q}{r-1} - \left(q + \frac{r-q}{r-1} \frac{w_n}{w_{nc}}\right) \exp\left(-\frac{w_t^2}{w_{tc}^2}\right) \right] \right\} \quad (3)$$

where w_{nc} and w_{tc} are crack opening displacements for mode I and II fracture respectively, W_1, r, q are intermediate variables and can be expressed as

$$W_1 = e p_n^u w_{nc}, \quad q = \sqrt{\frac{1}{2e} \frac{p_t^u w_{tc}}{p_n^u w_{nc}}}, \quad r = \frac{w_n^*}{w_{nc}} \quad (4)$$

where w_n^* is the normal opening displacement in correspondence of complete shear separation with $p_n = 0$ (a sort of 'measure of dilatancy'). Then the softening laws of interface variables in component forms are obtained with this free energy

$$p_n = -\frac{W_1}{w_{nc}} \exp\left(-\frac{w_n}{w_{nc}}\right) \left\{ \frac{w_n}{w_{nc}} \exp\left(-\frac{w_t^2}{w_{tc}^2}\right) + \frac{1-q}{r-1} \left[1 - \exp\left(-\frac{w_t^2}{w_{tc}^2}\right) \right] \left(r - \frac{w_n}{w_{nc}} \right) \right\} \quad (5)$$

$$p_t = -\frac{2W_1}{w_{nc}} \frac{w_t w_{nc}}{w_{tc}^2} \left(q + \frac{r-q}{r-1} \frac{w_n}{w_{nc}} \right) \exp\left(-\frac{w_n}{w_{nc}}\right) \exp\left(-\frac{w_t^2}{w_{tc}^2}\right) \quad (6)$$

Because no unloading is considered, softening laws obtained with free energy function can be interpreted as holonomic. Material parameters adopted in this model are

$$p_n^u, w_{nc}, p_t^u, w_{tc}, w_n^* \quad (7)$$

This model is presented on the basis of thermodynamics laws and its model parameters can be determined by a series of experimental results. It is of good ability in simulating experimental phenomenon of mixed-mode

fracture. Both decohesion and related dilatancy behaviours are accounted for in this model. Shortcomings of this model are: it requires rather many parameters to define the model, and some of these parameters can only be determined indirectly by an identification procedure. It is suitable for simulation of crack propagation of metals, not for static and/or quasi-static fracture analysis of concrete-like materials.

2.2 Elastoplastic Softening Interface: Coulomb-Type Cohesive Crack Models

Experimental results in references (see Hassanzadeh, 1990; Vutukuri, Lama and Saluja, 1974) showed that, failure modes of fracture specimen under mixed mode loading sometimes are path-dependent. Shear stress generates frictional slip (micro or macro), at the same time, results in dilatancy effect. The amount of dilatancy is influenced not only by material parameter, but also by normal pressure. Therefore, in this case, the behaviour of cohesive shear stress versus frictional slip (micro and/or macro) could not be taken as a material property. In many cases, wear and dilatancy, together with decohesion, are very important mechanism existing in the fracture of quasi-brittle materials. In recent years various Coulomb-type interface models have been proposed in the framework of plasticity to simulate the initiation and propagation of fracture under combined normal and shear stresses (Lotfi and Shing, 1994; Carol, Prat and Lopez, 1997). The basic assumption of such kind of models is that crack initiates once the stress reaches a 'yield surface', such as the Mohr-Coulomb criterion *etc.* During the propagation of the crack, the stress in cohesive zone remains on the yield surface, which shrinking (or say softening) until reaches a final state. Softening laws are described through evolution of failure criterion, instead of the traction-crack opening law.

Coulomb-type cohesive crack models are characterized by their various constitutive relationships for frictional sliding and dilatancy related to interface crack opening. Because procedures for analysis of various Coulomb-type cohesive models are the same in form, only their characteristics are summarised and compared in the following context.

2.2.1 Lotfi-Shing Model

Defining with s the tensile strength, c the cohesion, μ the internal friction coefficient, then the initial failure criterion of Lotfi-Shing model (Lotfi and Shing, 1994) was proposed as

$$F(\mathbf{p}, \mathbf{q}) = p_t^2 - \mu^2(p_n - s)^2 + 2r(p_n - s) = 0 \quad (8)$$

where $r = (c^2 - \mu^2 s^2) / 2s$ is the *radius* of curvature of a point on the yield surface, c is the shear strength under zero compression, s is the initial tensile strength, μ is the internal friction coefficient. Three parameters, $\{s, r, \mu\}$, which are regarded as *internal variables*, are adopted to describe the work-softening rules, i.e., the evolution of yield surface. Let \mathbf{q} denote the vector of internal variables

$$\mathbf{q} = \{s, r, \mu\} \quad (9)$$

The final state (marked by subscript "r") of \mathbf{q} is assumed to be

$$\mathbf{q}_r = \{0, 0, \mu_r\} \quad (10)$$

Their evolution laws were proposed as

$$\begin{aligned} s &= s_0 \left(1 - \frac{k_I}{G_f^I} - \frac{k_{II}}{G_f^{II}} \right) \\ r &= r_r + (r_0 - r_r) e^{-\beta \Delta III} \\ \mu &= \mu_r + (\mu_0 - \mu_r) e^{-\alpha \Delta III} \end{aligned} \quad (11)$$

where G_f^I, G_f^{II} are fracture energy for mode I and mode II crack respectively; α and β are material parameters; k_I, k_{II}, k_{III} are intermediate variables, which are functions of the rate of plastic displacement discontinuity $\dot{\mathbf{w}}^p$:

$$\begin{aligned} \dot{k}_I &= p_n H(p_n) \dot{w}_n^p, \quad \dot{k}_{II} = \dot{W}_2^{cr}, \quad \dot{k}_{III} = \dot{W}_3^{cr} \\ \dot{W}_2^{cr} &= [p_t - \bar{p}_t(\mathbf{p}, \mathbf{q})] \dot{w}_t^p, \quad \dot{W}_3^{cr} = \bar{p}_t(\mathbf{p}, \mathbf{q}) \dot{w}_t^p \end{aligned} \quad (12)$$

where $\bar{p}_t(\mathbf{p}, \mathbf{q})$ is the residual shear strength under the action of \mathbf{q} and is expressed as

$$\bar{p}_t(\mathbf{p}, \mathbf{q}) = \sqrt{\mu^2 p_n^2 - 2rp_n} \quad (13)$$

Plastic calculation can be carried out in the framework of conventional plasticity with non-associated flow rule. Potential function adopted in this model is

$$Q(\mathbf{p}, \mathbf{q}) = \eta p_t^2 + (r - r_r)(p_n - s) \quad (14)$$

where η is the dilatancy scaling parameter. Equations for calculation of relative displacements and traction and their rates are given as

$$\mathbf{w} = \mathbf{w}^e + \mathbf{w}^p, \quad \dot{\mathbf{w}}^p = \dot{\lambda} \frac{\partial Q}{\partial \mathbf{p}}, \quad \dot{\mathbf{p}} = \mathbf{D}^{ep} \dot{\mathbf{w}} \quad (15)$$

Except for those material parameters used in interface stiffness matrix \mathbf{D} , material parameters adopted in this model include

$$r_0, s_0, \mu_0, r_r, s_r, \mu_r, \eta, G_f^I, G_f^{II}, \alpha, \beta \quad (16)$$

Lotfi and Shing (1994) showed this model has good ability in simulating some experimental phenomena. Both decohesion and wear at interface can be considered by this model. As a counterpart of its high capability, this model requires up to 11 model parameters, some of which can only be determined experimentally and may be influenced by external loading conditions.

The dilatancy behaviour of this model is characterized by the parameter η . Because η is assumed as a material constant, which does not change in the fracture and frictional sliding process, the dilatancy amount in this model is not limited.

2.2.2 Carol-Prat- Lopez Model

With the same meaning of parameters s, c, μ as those used in Eqn. (8), the Carol-Prat- Lopez model adopts the following initial failure criterion

$$F(\mathbf{p}, \mathbf{q}) = p_t^2 - (c - \mu p_n)^2 + (c - s\mu)^2 = 0 \quad (17)$$

Carol-Prat- Lopez model adopts 3 model parameters, among which 2 of them are variables, to describe the evolution of the Coulomb type yield criterion given in Eqn. (17), they are collected in vector \mathbf{q} as:

$$\mathbf{q} = \{s, c, \mu\} \quad (18)$$

Final residual value of \mathbf{q} after degradation is given in this model as

$$\mathbf{q}_r = \{0, 0, \mu\} \quad (19)$$

Two internal variables, s and c , are involved in softening. Softening laws for these two internal variables were given as

$$s = s_0 \left[1 - S \left(\alpha_s, \frac{k_I}{G_f^I} \right) \right], \quad c = c_0 \left[1 - S \left(\alpha_c, \frac{k_I}{G_f^{IIa}} \right) \right] \quad (20)$$

where α_s and α_c are material parameters which set the shape of the exponential softening law; the expression of function S is

$$S(\alpha, \xi) = \frac{e^{-\alpha \xi}}{1 - (1 - e^{-\alpha}) \xi} \quad (21)$$

Only one intermediate variable k_I , which is a function of plastic opening rate, $\dot{\mathbf{w}}^p$, is used in above softening laws and its expression in rate form is

$$\dot{k}_I = p_n \dot{w}_n^p H(p_n) + p_t \dot{w}_t^p \left\{ 1 - \left| \frac{p_n \mu}{p_t} \right| [1 - H(p_n)] \right\} \quad (22)$$

where $H(*)$ is the Heaviside function.

Non-associated flow rule was adopted and the derivative of plastic potential function was given in the following equation

$$\dot{\mathbf{w}}^p = \dot{\lambda} \frac{\partial Q}{\partial \mathbf{p}}, \quad \frac{\partial Q}{\partial \mathbf{p}} = \left\{ \begin{array}{l} 2\mu(c - \mu p_n) f_p^{dil} f_c^{dil} \\ 2p_t \end{array} \right\} \quad (23)$$

where f_p^{dil} and f_c^{dil} are two functions which is adopted for simulation phenomenon of dilatancy. Definitions of these two functions are

$$f_p^{dil} = 1 - S \left(\alpha_p^{dil}, \left| \frac{p_n}{p_n^{dil}} \right| \right) [1 - H(p_n)], \quad f_c^{dil} = 1 - S \left(\alpha_c^{dil}, \frac{c}{c_0} \right) [1 - H(p_n)] \quad (24)$$

where p_n^{dil} is the critical value of compressive normal traction at which the dilatancy phenomena vanishes, and it is assumed as a material constant in this model.

Carol-Prat-Lopez model showed good prediction in simulating the real experimental results of mode I crack tests. However it appears some uncertainties in capturing the shear stress versus relative displacements as shown in Carol, Prat and Lopez (1997). This model requires 10 model parameters for simulation of dilatancy and softening behaviour except material parameters included in the interfacial elastic stiffness, i.e.,

$$r_0, s_0, \mu_0, p_n^{dil}, \alpha_s, \alpha_c, G_f^I, G_f^{II}, \alpha_c^{dil}, \alpha_p^{dil} \quad (25)$$

Carol-Prat-Lopez model has one model parameter less and 2 intermediary variables less than that of Lotfi-Shing model. The amount of numerical calculation required by this model is apparently less than the latter one.

Dilatancy behaviour of Carol-Prat-Lopez model was specialized by Eqn. (24). On the other hand, the amount of dilatancy is also limited by the critical normal compression p_n^{dil} , which is regarded as a material parameter by Carol, Prat and Lopez (1997).

Compared with Lotfi-Shing model, Carol-Prat-Lopez model has adopted two measures to specialize the dilatancy property of the model. On the aspect of the description of the shape evolution of the yield surface, Carol-Prat-Lopez model has made less effort than that of Lotfi-Shing model.

Both Lotfi-Shing model and Carol-Prat-Lopez model were established in the framework of incremental elasto-plasticity. In the theory of incremental plasticity, plastic strain is a vector of internal variables and is not allowed to decrease. Consequently, both these two models can not properly simulate the unloading process: crack closure. It will be shown numerical in the following section that the crack closure in this model will result in unreasonable high compression.

2.2.3 Piecewise Linear Interface Models for Mixed-Mode Cohesive Crack

On the basis of the works reported by Maier (1970), Bolzon, Maier and Novati (1994), Bolzon, Maier, Tin-Loi (1995), Cocchetti, Maier and Shen (2002) and Shen and Chen (2002) proposed Piecewise Linear (PWL) interface models for mixed-mode cohesive crack. PWL models aim at numerical simulation of quasibrittle fracture of concrete-like materials by Linear Complementarity Problems. Both holonomic and nonholonomic formulations were presented by Cocchetti Maier and Shen (2002) and Shen and Chen (2002).

In the following context, it is presented the simplest 5-plane PWL model, as shown in Figure 1. Both holonomic (i.e. total-quantity-form) and non-holonomic formulations (i.e. incremental form) are described.

An advantage of the PWL models is its broad scope of applications: it can be used for both holonomic formulation and non-holonomic formulation. In the opposite, explicit forms of cohesive laws, such as Xu-Needleman model, can only be used for the path-independent cases and unloading behaviour can not be considered. On the other side, the Lotfi-Shing and Carol-Prat-Lopez model can only be used in the incremental inelastic calculation.

(a) Holonomic formulation of the 5-plane PWL model

The matrix-form of Piecewise-Linear plastic yielding criteria for given traction vector \mathbf{p} is:

$$\varphi = \mathbf{N}^T \mathbf{p} - \mathbf{H}\boldsymbol{\lambda} - \mathbf{Y} \leq \mathbf{0} \quad (26)$$

The vector of yielding surfaces adopted in this model is

$$\varphi = \{\varphi_1 \quad \varphi_2 \quad \varphi_3 \quad \varphi_4 \quad \varphi_5\}^T \quad (27)$$

The vector of traction adopted in this model is

$$\mathbf{p} = \begin{Bmatrix} p_n \\ p_t \end{Bmatrix} \quad (28)$$

The vector of collection of normal direction of each yielding surface is

$$\mathbf{N} = \begin{bmatrix} 1 & \mu & \mu & 0 & 0 \\ 0 & 1 & -1 & 0 & 0 \end{bmatrix} \quad (29)$$

where \mathbf{N} is not unit matrix but only the matrix of outward normal directions of yielding surfaces. Relevant changes have been made on related terms simultaneously.

Vector of plastic multipliers is

$$\boldsymbol{\lambda} = \{\lambda_1 \quad \lambda_2 \quad \lambda_3 \quad \lambda_4 \quad \lambda_5\}^T \quad (30)$$

It is assumed that

$$\mathbf{w} = \mathbf{w}^e + \mathbf{w}^p \quad (31)$$

where \mathbf{w}^e and \mathbf{w}^p are elastic and plastic part of displacement respectively. If traction vector $\Delta\mathbf{p}$ is given as loading data, there is

$$\mathbf{w}^e = \mathbf{k}^{-1}\mathbf{p} \quad (32)$$

where \mathbf{k} is the elastic stiffness matrix at interface.

The plastic displacement vector is calculated by:

$$\mathbf{w}^p = \mathbf{V}\boldsymbol{\lambda} \quad (33)$$

Matrix \mathbf{V} in Eqn. (33) is the collection of the assumed plastic flow vectors of all the 5 yielding surfaces, and was expressed by Cocchetti, Maier and Shen (2002) and Shen and Chen (2002) as

$$\mathbf{V} = \begin{bmatrix} 1 & \mu_2 & \mu_2 & 0 & -\mu_2 \\ 0 & 1 & -1 & 0 & 0 \end{bmatrix} \quad (34)$$

where μ_2 is dilatancy-related coefficient.

According to the finite softening of strength parameters, the matrix of displacement softening modulus was obtained

$$\mathbf{H} = \begin{bmatrix} H_n & \frac{\chi_0}{c_0} H_t & \frac{\chi_0}{c_0} H_t & -H_n & -\frac{\chi_0}{c_0} H_t \\ \alpha H_n & H_t & H_t & -\alpha H_n & -H_t \\ \alpha H_n & H_t & H_t & -\alpha H_n & -H_t \\ H_n & \frac{\chi_0}{c_0} H_t & \frac{\chi_0}{c_0} H_t & -H_n & -\frac{\chi_0}{c_0} H_t \\ \alpha H_n & H_t & H_t & -\alpha H_n & -H_t \end{bmatrix} \quad (35)$$

where χ_0 is the initial tensile strength, c_0 is the initial shear strength, H_n and H_t are the softening modulus in normal and tangential directions respectively, α is the influence parameter of normal crack opening on tangential crack opening.

The vector of initial strength parameters of both tension and shear behaviour is

$$\mathbf{Y} = \{\chi_0 \quad c_0 \quad c_0 \quad \chi_0 \quad c_0\}^T \quad (36)$$

In the above equations, material constants model parameters are:

$$\mu, \mu_2, \alpha, c_0, \chi_0, G_f^I, G_f^{II}, H_n, H_t \quad (37)$$

Linear Complementarity Problems of vector $\boldsymbol{\varphi}$ and vector $\boldsymbol{\lambda}$ for given displacement vector \mathbf{w} are

$$\boldsymbol{\varphi} = \mathbf{N}^T \mathbf{k} \mathbf{w} - (\mathbf{N}^T \mathbf{k} \mathbf{V} + \mathbf{H}) \boldsymbol{\lambda} - \mathbf{Y} \leq \mathbf{0} \quad (38)$$

$$\boldsymbol{\varphi} \leq \mathbf{0}, \quad \boldsymbol{\lambda} \geq \mathbf{0}, \quad \boldsymbol{\varphi}^T \boldsymbol{\lambda} = 0 \quad (39)$$

These Linear Complementarity Problems of vector $\boldsymbol{\varphi}$ and vector $\boldsymbol{\lambda}$ can be solved by a method of mathematical programming, as that described by Bolzon, Maier and Novati (1994), Bolzon, Maier, Tin-Loi (1995).

(b) Nonholonomic formulation

For the case of complicated external loading conditions, holonomic plastic theory can not meet the needs of accuracy requirement. Consequently nonholonomic formulation becomes necessary.

Even for the nonholonomic case, it was also assumed that all the fundamental relationships for the coupling between fracture process and Piecewise Linear cohesive relations expressed in Eqns. (31) to (36) always holds, but the following incremental relationships have to be adopted instead of their counterparts in holonomic formulation, i.e.,

$$\boldsymbol{\varphi} = \mathbf{N}^T (\mathbf{p}^0 + \Delta\mathbf{p}) - \mathbf{H} (\boldsymbol{\lambda}^0 + \Delta\boldsymbol{\lambda}) - \mathbf{Y}^0 \leq 0 \quad (40)$$

Eqn. (40) means that the traction points on the consequent softening yielding surface is loading-path-dependent. And, it was assumed

$$\Delta\mathbf{w} = \Delta\mathbf{w}^e + \Delta\mathbf{w}^p \quad (41)$$

If incremental traction vector $\Delta\mathbf{p}$ is given as loading data, there is

$$\Delta\mathbf{w}^e = \mathbf{k}^{-1} \Delta\mathbf{p} \quad (42)$$

$$\Delta\mathbf{w}^p = \mathbf{V} \Delta\boldsymbol{\lambda} \quad (43)$$

As incremental displacement discontinuity vector $\Delta\mathbf{w}$ is given as input data, there is

$$\Delta\mathbf{p} = \mathbf{k} (\Delta\mathbf{w} - \mathbf{V} \Delta\boldsymbol{\lambda}) \quad (44)$$

By analogy to subsection 2.1.1, it can be written the following nonholonomic LCP formulation for given incremental traction vector $\Delta \mathbf{p}$ as loading condition:

$$\varphi = \mathbf{N}^T (\mathbf{p}^0 + \Delta \mathbf{p}) - \mathbf{H}(\boldsymbol{\lambda}^0 + \Delta \boldsymbol{\lambda}) - \mathbf{Y}^0 \leq \mathbf{0} \quad (45)$$

$$\varphi \leq \mathbf{0}, \quad \Delta \boldsymbol{\lambda} \geq \mathbf{0}, \quad \varphi^T \Delta \boldsymbol{\lambda} = 0 \quad (46)$$

and for given incremental displacement discontinuity vector $\Delta \mathbf{w}$ as loading condition, the Linear Complementarity Problems of vector φ and vector $\Delta \boldsymbol{\lambda}$ for given displacement vector $\Delta \mathbf{w}$ are

$$\varphi = \mathbf{N}^T (\mathbf{p}^0 + \mathbf{k} \Delta \mathbf{w}) - (\mathbf{N}^T \mathbf{k} \mathbf{V} + \mathbf{H}) \Delta \boldsymbol{\lambda} - (\mathbf{H} \boldsymbol{\lambda}^0 + \mathbf{Y}^0) \leq \mathbf{0} \quad (47)$$

$$\varphi \leq \mathbf{0}, \quad \Delta \boldsymbol{\lambda} \geq \mathbf{0}, \quad \varphi^T \Delta \boldsymbol{\lambda} = 0 \quad (48)$$

where superscript "0" denotes the values of the variables at the starting state of the incremental loading. These Linear Complementarity Problems can also be solved by a method of mathematical programming as described by Bolzon, Maier., Tin-Loi (1995).

The dilatancy behaviour of this Piecewise Linear (PWL) model with 5-plane is specialized by the matrix \mathbf{V} in Eqn. (34). It is shown in the next section by numerical examples that the dilatancy behaviour of the PWL model is limited by the softening process of shear strength, and the maximum of dilatancy is a finite value.

One of the numerical disadvantages of the PWL models is its multiplicity of solutions at the softening branch of a \mathbf{p} - \mathbf{w} diagram, as that illustrated and discussed by Cocchetti Maier and Shen (2002) through a 7-plane model.

2.3 Corigliano-Bolzon's Interface Model for Quasi-Brittle Fracture in Composites

As an alternative tool to describe the elastoplastic interface cohesive model with Coulomb type models, Corigliano (1993) and Bolzon and Corigliano (1997) presented their model in the so-called *standard dissipative system* for cohesive interface crack. Interface of thickness t is assumed *a priori* existed and is the loci of crack propagation. The general description of elasto-plastic constitutive relationships for cohesive interface variables were presented by Corigliano (1993) and Bolzon and Corigliano (1997) as follows:

$$\begin{cases} \mathbf{w} = \mathbf{w}^e + \mathbf{w}^p \\ \mathbf{p} = \frac{\partial \Psi(\mathbf{w}^e, \boldsymbol{\alpha})}{\partial \mathbf{w}^e}, \quad \mathbf{a} = \frac{\partial \Psi(\mathbf{w}^e, \boldsymbol{\alpha})}{\partial \boldsymbol{\alpha}} \\ \dot{\mathbf{w}}^p = \dot{\lambda} \frac{\partial f^T(\mathbf{p}, \mathbf{a})}{\partial \mathbf{p}}, \quad \dot{\boldsymbol{\alpha}} = \dot{\lambda} \frac{\partial f^T(\mathbf{p}, \mathbf{a})}{\partial \mathbf{a}} \end{cases} \quad (49)$$

where $\boldsymbol{\alpha}$ denotes the vector of internal variables, \mathbf{a} denotes the vector of conjugate force corresponding to $\boldsymbol{\alpha}$; Ψ is the free energy function for a point on the cohesive interface. The expression of free energy function was given by Corigliano (1993) as

$$\Psi = \frac{1}{2} [K_n (w_n^e)^2 + K_{t1} (w_{t1}^e)^2 + K_{t2} (w_{t2}^e)^2] + \Psi_2(\boldsymbol{\alpha}) \quad (50)$$

where K_x , $x = n, t1, t2$, denotes elastic stiffness in the normal and two tangential directions respectively for a 3-dimensional problem, $\Psi_2(\boldsymbol{\alpha})$ is an additional function to set the shape of softening law in \mathbf{p} - \mathbf{w} space. As assume α as a scalar and given

$$\Psi_2(\alpha) = \alpha + \frac{1}{2} h \alpha^2 \quad (51)$$

where h is a positive non-dimensional softening parameter, then nonlinear softening branch can be obtained as shown in Figure 2.

2.3.1 Elastoplastic Damage Interface Model

For the elasto-plastic damage interface model, the activation function of inelastic processes on the cohesive interface was expressed by Corigliano (1993) and Bolzon and Corigliano (1997) as:

$$F = \sqrt{a_n \left(\frac{\langle p_n \rangle_+}{1-d_n} \right)^2 + a_{t1} \left(\frac{p_{t1}}{1-d_{t1}} \right)^2 + a_{t2} \left(\frac{p_{t2}}{1-d_{t2}} \right)^2} - 1 + h \lambda \quad (52)$$

$$a_i = \frac{1}{(p_{ic})^2}, \quad i = n, t1, t2 \quad \text{respectively}$$

where $\langle \bullet \rangle_+$ denotes only the positive case of the variable in the bracket is accounted for, d_n, d_{t1}, d_{t2} are damage variables, p_{ic} denotes the critical traction value at which softening begin to occur in that i th direction. The degradation of stiffness K_i at interface caused by damage was considered in this model, and the free energy for damaged interface point is

$$\Psi = \frac{1}{2}(1-d_n)K_n \langle w_n \rangle_+^2 + \frac{1}{2}K_n \langle w_n \rangle_-^2 + \frac{1}{2}(1-d_{t1})K_{t1}w_{t1}^2 + \frac{1}{2}(1-d_{t2})K_{t2}w_{t2}^2 \quad (53)$$

where subscript '+' denotes tensional state and '-' denotes compressive state. In this model, unified flow surface was adopted for all irreversible processes, i.e., damage and plasticity *etc.* The evolution laws for damage and plasticity were given as

$$\begin{cases} \dot{\mathbf{w}}^p = \frac{\partial F}{\partial \mathbf{p}} \dot{\lambda}, & \dot{\lambda} = \sqrt{(\dot{\mathbf{w}}^p)^T \cdot (\dot{\mathbf{w}}^p)} \\ \mathbf{d} = \mathbf{L}(h\lambda) = \begin{cases} 1 - \sqrt{1 - 2\gamma_n h \lambda} \\ 1 - \sqrt{1 - 2\gamma_{t1} h \lambda} \\ 1 - \sqrt{1 - 2\gamma_{t2} h \lambda} \end{cases} \\ F \leq 0, F \dot{\lambda} = 0, \dot{\lambda} \geq 0 \end{cases} \quad (54)$$

where $\gamma_n, \gamma_{t1}, \gamma_{t2}$ are model parameters and can be determined by classical fracture energy through the following equations:

$$\begin{cases} G_I = \frac{1}{K_n a_n} \left(\frac{1}{2} + \frac{1}{15\gamma_n^2} + \frac{1}{3\gamma_n} \right) + \frac{1}{8\gamma_n^2 h} + \frac{1}{2\gamma_n h} \\ G_{II} = \frac{1}{K_t a_t} \left(\frac{1}{2} + \frac{1}{15\gamma_t^2} + \frac{1}{3\gamma_t} \right) + \frac{1}{8\gamma_t^2 h} + \frac{1}{2\gamma_t h} \end{cases} \quad (55)$$

where γ_t denotes both γ_{t1} and γ_{t2} .

There are 10 parameters being adopted in this model for 3-dimensional problems: $K_i, \alpha_i, \gamma_i, i = n, t1, t2$ and h . Experimentally speaking, this method (i.e. unified flow rule for damage and plasticity) is a kind of reasonable approximation of physical reality, but it is not a general proper way of dealing with plural dissipative process.

In the process of crack closure and re-open, the stiffness is degraded to a certain value depending on the extent of the cohesive fracture. It is shown in the following section by numerical example that the influence of damage on the cohesive interface model.

Interface models formulated in the so-called *standard dissipative system* by Corigliano (1993) and Bolzon and Corigliano (1997) showed good ability in simulating softening behaviour of both strength and stiffness. The number of parameters used in the description of the softening constitutive relationship is much less than that used by Coulomb-type Lotfi-Shing model and Carol-Prat-Lopez model. Dilatancy properties were not discussed explicitly by existing applications (see Corigliano, 1993; Bolzon and Corigliano, 1997). According to Rice's internal variable theory (Rice, 1971), dilatancy, in the sense of inelastic volume increase, can be explicitly connected with damage evolution, which usually corresponds to increase of crack opening and crack propagation.

3. NUMERICAL TESTS OF SELECTED INTERFACE MODELS

Models selected from those introduced in above sections, both holonomic and nonholonomic, have been implemented in a set of subroutines of constitutive models for 2D analysis for the purpose of model verification. These subroutines can carry on the displacement-traction type calculations.

In the following context, mode I and mode II responses are checked the first for each selected model. For mixed mode failure, the input displacement loading path $\mathbf{w}=\mathbf{w}(t)$ is illustrated the first, and it is followed by consequent output $\mathbf{p}(t)-\mathbf{w}(t)$ response, which is shown in the form of $\mathbf{p}(t)-\mathbf{w}(t)$ diagram. For more complicated cases, immigration traces of traction points corresponding to a displacement loading up to failure (detachment and/or free movement) are illustrated as well.

3.1 Numerical Tests of Xu-Needleman Cohesive Interface Model

Firstly, the fundamental behaviours of both mode I and mode II displacement loading are performed for Xu-Needleman model. Values of parameters in these calculations are adopted as:

$$p_n^u = 2.8 \text{MPa}, p_t^u = 7.0 \text{MPa}, w_{nc} = 0.014 \text{mm}, w_{tc} = 0.035 \text{mm}, w_{nc}^* = 0.01 \text{mm}$$

Figure 3a indicates that the mode I behaviour of Xu-Needleman model is properly described, but Figures 3b indicates that the model behaviour for mode II displacement loading is not reasonable: the shear displacement has resulted in too much compression in normal direction. It indicates that the dilatancy property of this model is not reasonable.

Figure 4 shows the model response under mixed-mode displacement loading. Although the mode II behaviour is not reasonable, the dilatancy response of Xu-Needleman model under mixed-mode loading is reasonable. This indicates that Xu-Needleman model can be used for those cases of mixed-mode interface fracture at which the mode I crack is the dominant factor.

3.2 Numerical Tests of Carol-Prat-Lopez Model

Parameter values are adopted as: elastic stiffness $K_n = K_t = 200 \text{MPa} / \text{mm}$; frictional angle $\phi = \arctan(0.9)$, $\mu = 0.9$; tensile strength $s_0 = 2.8 \text{MPa}$, shear strength $c_0 = 7.0 \text{MPa}$; fracture energy for mode I crack $G_f^I = 0.1 \text{N} / \text{mm}$, for mode II crack $G_f^{II} = 1.0 \text{N} / \text{mm}$; other parameters are $\alpha_s = 0.$, $\alpha_c = 1.5$, $\alpha_p^{dil} = 2.7$, $\alpha_c^{dil} = 3.$, $p_n^{dil} = 56 \text{MPa}$.

Figure 5a indicates that the mode I behaviour of Carol-Prat-Lopez model is properly described. Figure 5b shows the dilatancy behaviour of Carol-Prat-Lopez model under mode II displacement loading. It is a reasonable phenomenon that the normal compression increase with the development of the inelastic mode II shear crack opening. With the increase of the shear displacement loading, the increase of compression tends to be less and less in a nonlinear way, which indicates that the saturation of dilatancy is going to be reached.

Figure 6b displays the situations of the immigration of the traction points corresponding to a set of mixed-mode displacement loading paths. With the increase of the inelastic shear component of displacement loading, dilatancy property results in compression in the normal direction. As the end of the fracture in shear direction is reached, the dilatancy stop to increase, the final frictional Mohr-Coulomb state is formed. Afterwards, with the increase of the normal component of the displacement loading, the normal compression at interface starts to decrease.

It is clearly indicated in Figure 7b the unloading behaviour of Carol-Prat-Lopez model: crack closure is not permitted by the model because of the plastic crack opening is irreversible. The crack closure in normal direction results in high compression. This is an important shortcoming of this model, particularly when this model is used for the dynamic analysis of concrete structures, at where the cyclic loading condition is essential.

3.3 Numerical Tests of Piecewise Linear (PWL) Cohesive Interface Crack Model

Both of the holonomic and nonholonomic versions of the PWL interface model are tested numerically in this section. The LCP problems of the piecewise linear cohesive interface crack model are solved by using the mathematical programming solver, the PATH-Solver. The descriptions on the principle of the PATH-Solver can be found in the articles by Bolzon, Maier., Tin-Loi (1995) and Dirkse and Ferris (1995).

Parameter values are given based on those adopted in Carol-Prat-Lopez model, they are: $K_n = K_t = 200 \text{MPa} / \text{mm}$, $\phi = \arctan(0.9)$, $\mu = \mu_2 = 0.9$; $\chi_0 = 2.8 \text{MPa}$, $c_0 = 7.0 \text{MPa}$; $G_f^I = 0.1 \text{N} / \text{mm}$, $G_f^{II} = 1.0 \text{N} / \text{mm}$; coupling coefficient parameter $\alpha = 0.8$.

For the monotonic loading case, the numerical solutions obtained by the holonomic PWL model are the same as the solutions that obtained by nonholonomic one. Figure 8a shows the response of PWL interface model under mode II displacement loading. It is seen that the dilatancy of the model comes to its maximum as the fracture in shear is completed, and afterwards, no more increase of the compression in normal direction, and the traction state keeps on the final frictional Mohr-Coulomb relationship.

Figure 8b displays the immigration of the traction points corresponding to $\theta = 30^\circ$ mixed-mode displacement loading paths, as that shown in Figures 6a and 6b. Similar to the case in Carol-Prat-Lopez model, dilatancy property results in compression in the normal direction in a linear manner, which results in the traction point immigrate to the negative direction of the normal component traction linearly. As the end of the fracture in shear direction is reached, the dilatancy stop to increase, the final frictional Mohr-Coulomb state is formed. Afterwards, with the increase of the normal component of the displacement loading, the normal compression at interface starts to decrease up to detachment state in a linear way as well.

Figure 9b shows the cyclic response of the PWL cohesive model under mode II cyclic loading. It is seen in Figure 9b that as the elasto-plastic loading up to point *a* in Figure 9a being applied, there are corresponding points *a* appear in Figure 9b and Figure 9c. As the reverse displacement loading being applied reaches point *b* in Figure

9a, it is seen in Figure 9b that the cohesive fracture is completed and the final Coulomb state is reached. The increase of shear displacement will cause no further dilatancy thereafter.

For the nonholonomic version of the PWL model, because it is built in the framework of incremental plasticity, the decrease of plastic displacement, i.e. crack closure, is also not permitted to occur. This behaviour of the PWL model is similar to that of Carol-Prat-Lopez model.

3.4 Numerical Tests of Corigliano-Bolzon's Elastoplastic-Damage Cohesive Interface Model

In this calculation, 10 parameters are used for 3-dimensional problems (subscript 1, 2, 3 indicate the directions of n , t_1 and t_2 respectively). Their values are given as the following based on the values of parameters used in above context:

$k_1=200\text{MPa/mm}$, $k_2=200\text{MPa/mm}$, $k_3=200\text{MPa/mm}$, $a_1=0.13$, $a_2=0.13$, $a_3=0.3$, $\gamma_1=0.01$, $\gamma_2=0.024$, $\gamma_3=0.024$, $h=0.256$.

Figure 10a shows the response of this interface model under mode I displacement loading and unloading. It is seen that the mode I phenomenon is properly reproduced. In the unloading process, the damage-caused degradation of stiffness is also accounted for in this model. This is an important factor for dynamic analysis: less stiffness will result in less resistance during unloading, except other issues related to stiffness degradation.

Figure 10b shows the response of this interface model under mode II displacement loading. Because it is designed in this model that the complete of the shear softening is determined by the de-cohesion process in normal direction, the behaviour shown here is rather 'brittle'.

Figure 11a shows the mixed-mode response. The displacement loading path of $\theta=30^\circ$ shown in Figure 6a is applied. At this mixed-mode loading case, the fracture behaviour in normal direction is properly reproduced, and the fracture in tangential direction is rather brittle, no dilatancy appears in this case.

Figure 11b shows the situations of immigration of traction points corresponding to the 3 kind of loading paths given in Figure 6a. It is seen that plastic displacement in tangential direction does not cause any compression in normal direction. This indicates that: this model doesn't consider the dilatancy phenomenon.

4. CONCLUSION AND ENDING REMARKS

With the numerical tests given before, it can be concluded that:

- (1) Xu-Needleman model is not suitable for quasi-brittle fracture analysis of concrete-like materials.
- (2) Carol-Prat-Lopez model is a good model for fracture analysis of concrete-like material. It has the 4 required properties mentioned above. But it also has a few shortcomings: (a) the limit of dilatancy is introduced by a given bound of compressive traction in normal direction. This is true for some cases, but not general is. The value of pressure threshold for this phenomenon is also not a material constant, but a parameter that varies with different external loading conditions.
- (3) Piecewise linear interface model can properly simulate mixed-mode interface fracture and interfacial frictional behaviour. In this model, dilatancy is modeled by nonassociated flow rule and its limit is designed to reach simultaneously with the end of softening process in shear direction. Formulations as Linear Complementarity Problems are given on the purpose of solving this problem with mathematical programming method. Because of its linearity, the holonomic version of this model can be used in the calculations of *direct method*, such as plastic limit analysis, of a concrete structure. Its nonholonomic version can be used in the incremental analysis under complicated loading conditions.

Numerical tests indicate its reasonable ability in reproducing the mixed-mode cohesive fracture, and the corresponding dilatancy behaviour.

- (4) Corigliano-Bolzon's elastoplastic damage cohesive interface model showed its good ability in reproducing the softening phenomenon in fracture process, and unloading behaviour. But it is clear that it can not be directly used for description of frictional sliding on the interface without further improvement because of its dilatancy property.

In summary, it can be said that, piecewise linear elastoplastic interface model for mixed-mode interface fracture is the most suitable model for description of quasi-brittle fracture of concrete-like materials, and is the only model suitable for shakedown and limit analysis of structures that dominated by mixed-mode interface cracks. Furthermore, the damage behaviour as that shown by Corigliano-Bolzon model, should also be comprised in this constitutive model in order to make it more suitable for a quasi-static fracture analysis.

ACKNOWLEDGEMENTS

Thanks are due to the NNSF of China for the financial support via contract no. 10472072, and to the Department of Education, Liaoning Province, China, for the financial support via contract no. 2005C035.

REFERENCES

- Bazant Z. P., Cedolin L., (1991), "Stability of Structures: Elastic, Inelastic, Fracture and Damage Theories", Oxford University Press, Oxford, New York.
- Karihaloo B. L., (1995), "Fracture Mechanics and Structural Concrete", Longman Scientific & Technical, Harlow, Great Britain.
- Hassanzadeh, M., (1990), Determination of fracture zone properties in mixed mode I and II, *Engrg. Fracture Mech.*, **35**(4/5): 845–853.
- Vutukuri, V. S., Lama, R. D. Saluja, S. S. , 1974, "Handbook on Mechanical Properties of Rocks", Vol.1, Berlin: Trans Tech Publisher.
- Camacho, G.T., Ortiz M., (1996), Computational modeling of impact damage in brittle materials. *Inter J. Solids Struct.*, **33**(20-22): 2899-2938.
- Xu X., Needleman A., (1994), Numerical simulation of fast crack growth in brittle solids, *J. Mech. Phys. Solids*, **42**(7): 1397–1434.
- Lotfi, H., Shing, P., (1994), Interface model applied to fracture of masonry structures, *J. Engng. Mech., ASCE*, **120**(1): 63-80.
- Carol, I., Prat, P.C., and Lopez, C.M., (1997), Normal/shear cracking model: application to discrete crack analysis, *J. Engng. Mech., ASCE*, **123**(1): 1-9.
- Cocchetti G., Maier G. and Shen X. P., (2002), On piecewise linear models of interfaces and mixed mode cohesive cracks. *Computer Modeling in Engineering and Sciences*, **3**(3): 279-298.
- Shen, Xinpu, (2001), A piecewise linear elasto-plastic constitutive model for mixed mode interface cracks. *Chinese J. Geotech Engng (English article)*, **23**(2), 250-256.
- Corigliano A., (1993), Formulation, identification and use of interface models in the numerical analysis of composite delamination. *Int. J. Solids Struct.*, **30**(20), 2779-2811.
- Bolzon G., Corigliano A., (1997), A discrete formulation for elastic solids with damaging interfaces. *Comp. Methods Appl. Mech. Engng.*, **140**(2): 329-359.
- Maier, G., (1970), A matrix structural theory of piecewise-linear plasticity with interacting yield planes, *Meccanica*, **5**(1): 55-66.
- Bolzon, G., Maier, G., Novati G., (1994), Some aspects of quasi-brittle fracture analysis as a linear complementarity problem, *Fracture and Damage in Quasibrittle Structures*, Z. P. Bazant, Z. Bittnar, M. Jirasek, J. Mazars Eds., E & FN Spon, London, 159-174.
- Bolzon G., Maier G., Tin-Loi F., (1995), Holonomic and non-holonomic simulation of quasi -brittle fracture: a comparative study of mathematical programming approaches. In: *Fracture Mechanics of Concrete Structures*, Wittman F. H. (Ed.), Aedificatio Publishers, Freiburg, 885-898.
- Shen, Xinpu, Lixin Chen, (2002), Investigation on mixed-mode cohesive crack in the presence of water pressure for interface between dam and its foundation. *Advances in Structural Engineering*, **5**(1): 45-52.
- Corigliano A., Allix O., (2000), Some aspects of interlaminar degradation in composites. *Comput. Methods Appl. Mech. Engng.*, **185**:203-224.
- Rice, R. J., (1971), Inelastic constitutive relations for solids: an internal variable theory and its application to metal plasticity. *J. Mech. Phys. Solids*, **19**, 443-455.
- Dirkse S.P., Ferris M.C., (1995), The PATH solver: a non-monotone stabilisation scheme for mixed complementarity problems, *Optimization Methods & Software*, **5**, 123–156.

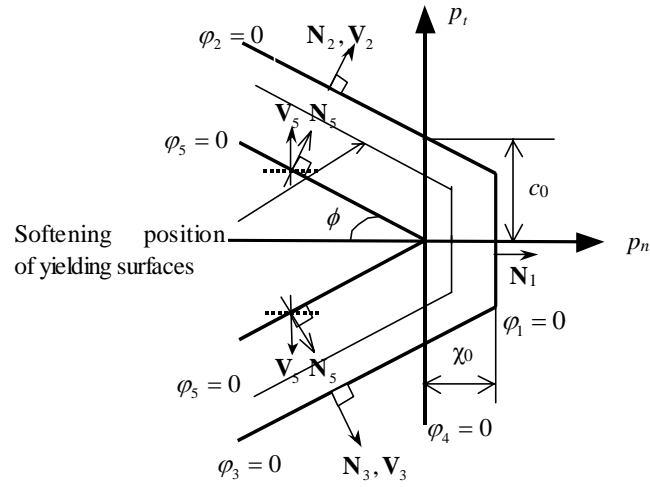


Figure 1 Illustration of piecewise-linear plastic yielding surfaces (5-plane model).

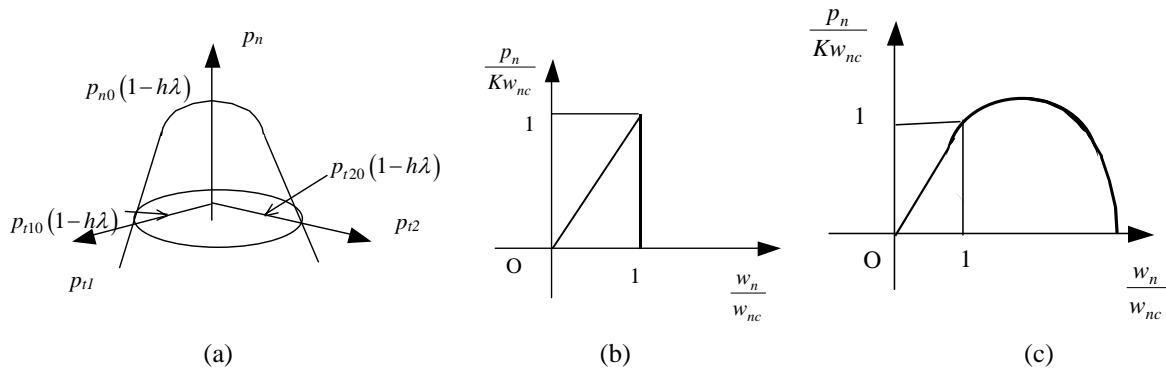


Figure 2 Illustration of Corigliano-Bolzon model: (a) Initial elastic domain, (b) brittle failure, and (c) progressive failure.

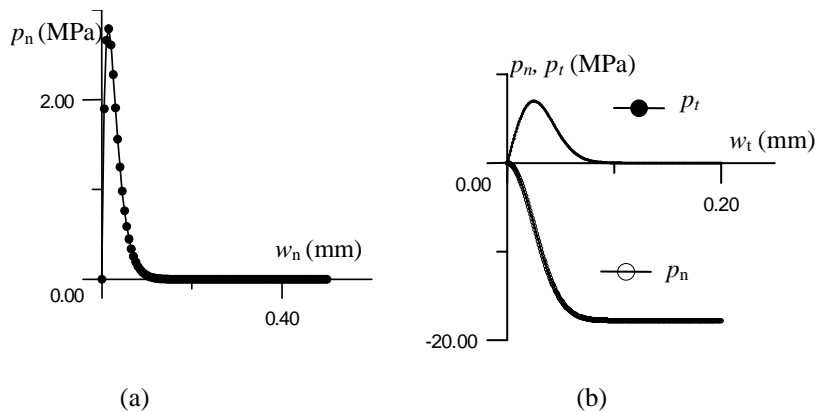


Figure 3 Numerical verification of Xu-Needleman model: (a) Mode I behaviour: p_n - w_n response, (b) Mode II behaviour: variation of p_n and p_t versus w_t .

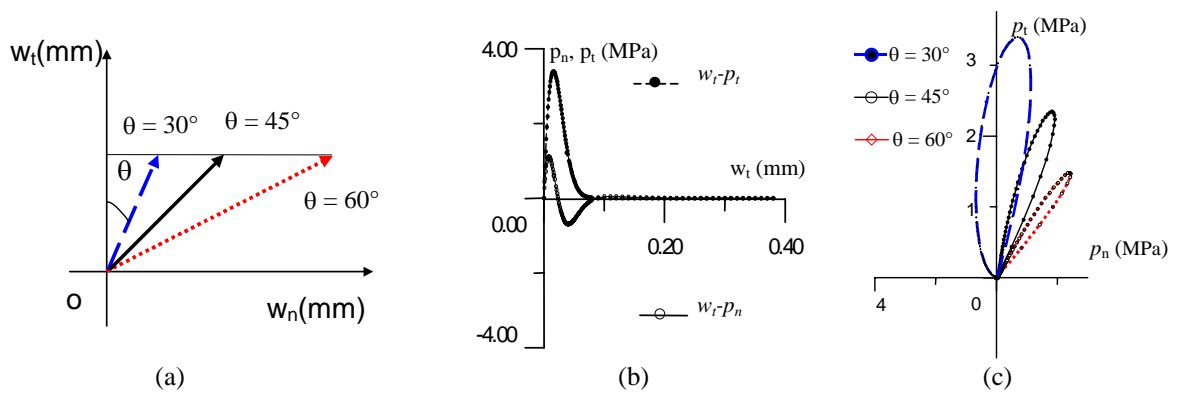


Figure 4 Numerical verification of Xu-Needleman model: Mixed-mode behaviours: (a) displacement loading paths; (b) variation of p_n and p_t versus w_t ($\theta=30^\circ$). (c) evolution of traction states for different loading angles.

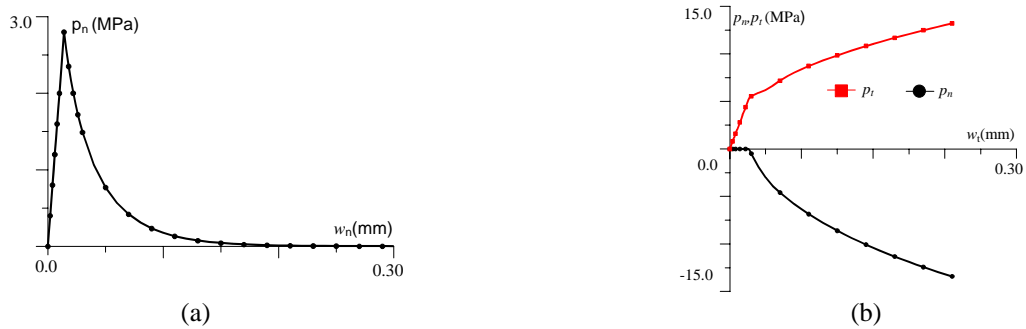


Figure 5 Numerical verification of Carol-Prat-Lopez model: (a) Mode I displacement loading: p_n - w_n response, (b) Mode II loading: response of w_t - p_n and w_t - p_t .

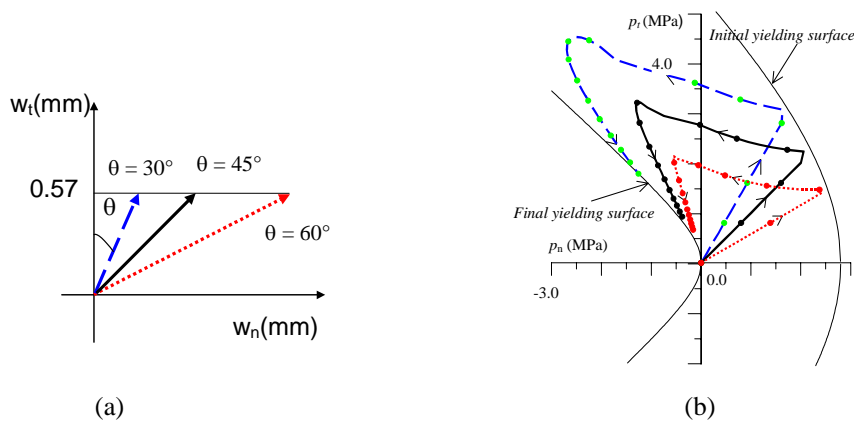


Figure 6 Numerical verification of Carol-Prat-Lopez model: (a) loading paths; (b) evolution of traction states.

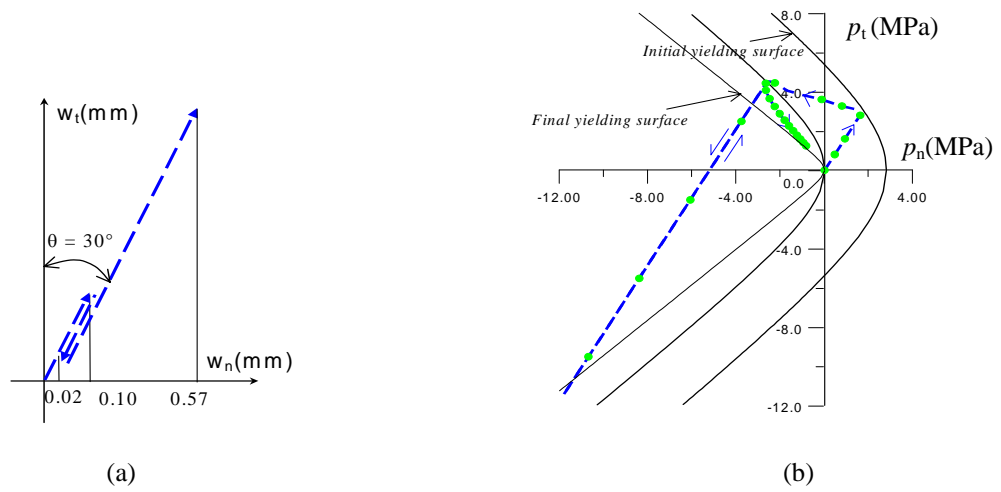


Figure 7 Numerical verification of Carol-Prat-Lopez model: (a) mixed mode variable loading path; (b) evolution of traction states.

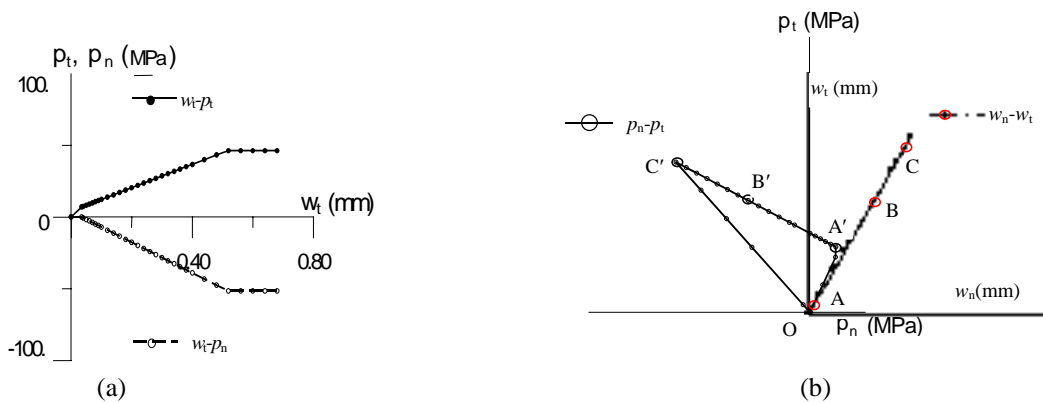


Figure 8 Numerical verification of Piece-Wise Linear model: (a) Mode II loading: p_n-w_t and p_t-w_t response. (b) evolution of traction states (A' , B' , C') and their corresponding displacement states (A , B , C) (mixed mode $\theta=30^\circ$).

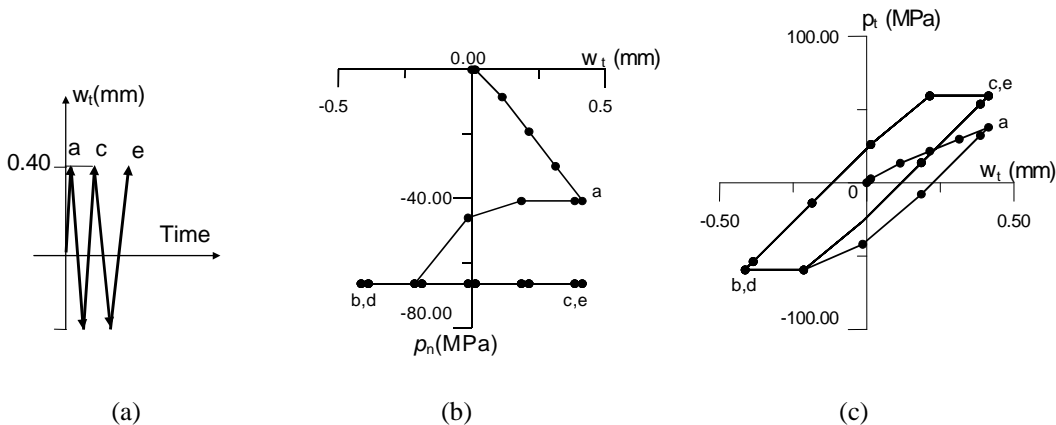


Figure 9 Cyclic response of Piece-Wise Linear model: (a) mode II displacement loading; (b) p_n-w_t response; (c) p_t-w_t response.

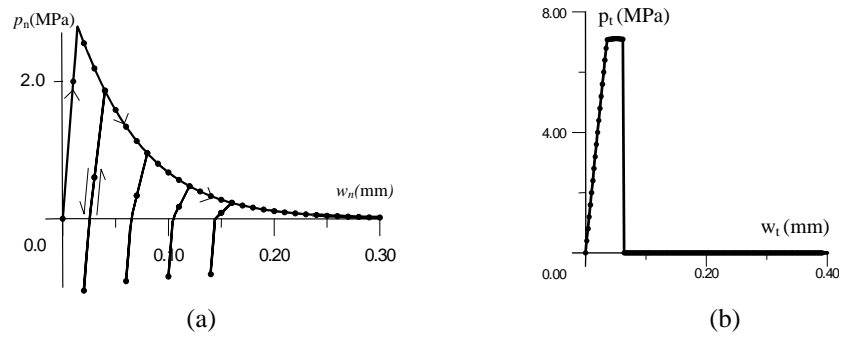


Figure 10 Numerical verification of Corigliano-Bolzon model: (a) Mode I response: loading and unloading; (b) Mode II response: variation of p_t versus w_t .

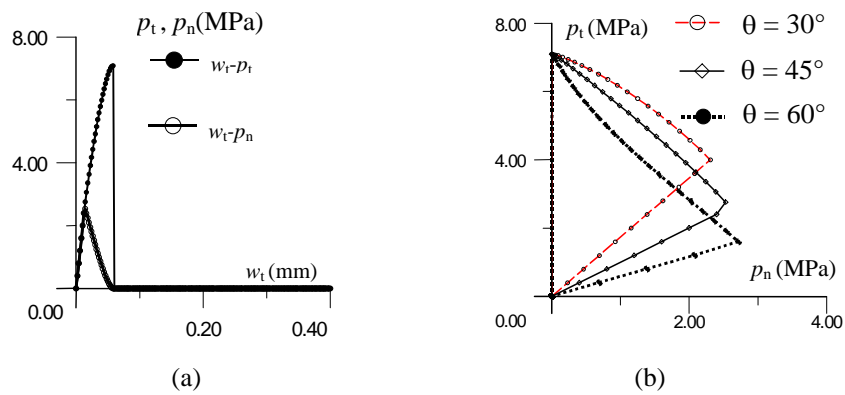


Figure 11. Mixed mode response ($\theta=30^\circ$) of Corigliano-Bolzon model: (a) variation of p_n versus w_t and p_t versus w_t ; (b) comparison of results for different loading path: evolution of traction states.